2D Electrostatic Actuation of Microshutter Arrays

Authors: Devin E. Burns, Lance H. Oh, Mary J. Li, Justin S. Jones, Daniel P. Kelly, Yun Zheng, Alexander S. Kutyrev, Samuel H. Moseley

Abstract

An electrostatically actuated microshutter array consisting of rotational microshutters (shutters that rotate about a torsion bar) were designed and fabricated through the use of models and experiments. Design iterations focused on minimizing the torsional stiffness of the microshutters, while maintaining their structural integrity. Mechanical and electromechanical test systems were constructed to measure the static and dynamic behavior of the microshutters. The torsional stiffness was reduced by a factor of four over initial designs without sacrificing durability. Analysis of the resonant behavior of the microshutter arrays demonstrates that the first resonant mode is a torsional mode occurring around 3000 Hz. At low vacuum pressures, this resonant mode can be used to significantly reduce the drive voltage necessary for actuation requiring as little as 25V. 2D electrostatic latching and addressing was demonstrated using both a resonant and pulsed addressing scheme.

Introduction

Rotational microshutters are transmissive light apertures with unparalleled open/close contrast (>10,000) compared to other optical MEMS devices and high fill factors (>70%) compared to other high throw actuators [(1), (2)]. NASA developed rotational microshutters for the James Webb Space Telescope's (JWST) NIRSpec detector to enable scientists to select specific objects within the field of view (multi-object spectroscopy), improving the efficiency of the detector more than 100 times.

The ability to individually select objects within the field of view requires a method to open specific microshutters. This is accomplished through a 2-D addressing scheme (referred to as 2-D addressing because electrodes run in columns and rows forming a 2-D matrix). For JWST, NASA elected to use a combination of magnetic actuation via a scanning bulk magnet and electrostatic latching via front and back electrodes to achieve 2-D addressing [(1) (2)]. Motohara et al. [(3)] have demonstrated 1-D electrostatic actuation by applying a DC signal to front electrodes.

In this work, microshutter arrays were developed to achieve 2-D addressing using only electrostatic forces. This development effort focused on producing microshutters that could be actuated reliably using minimal actuation voltages. To support the development effort, custom mechanical and electromechanical test systems were constructed for static and dynamic characterization of the microshutters. The experimental effort was also used to support a modeling effort aimed at better understanding the electromechanical response of the microshutters. Two 2-D electrostatic addressing schemes were demonstrated using AC resonant and DC pulsed actuation respectively.

Procedures

Microshutters were fabricated from silicon on insulator (SOI) wafers using a combination of surface and bulk micromachining. As shown in

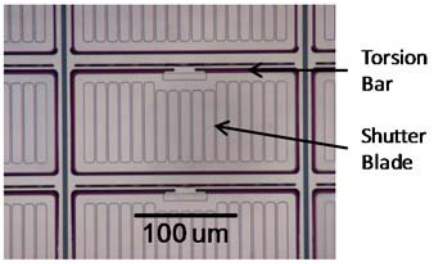

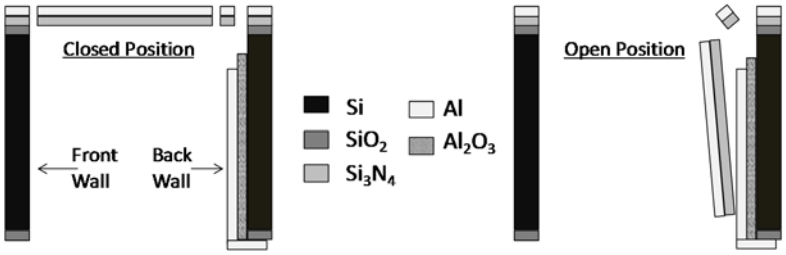

Figure 1(a), microshutters consist of a long torsion bar and a shutter blade. In the closed position (

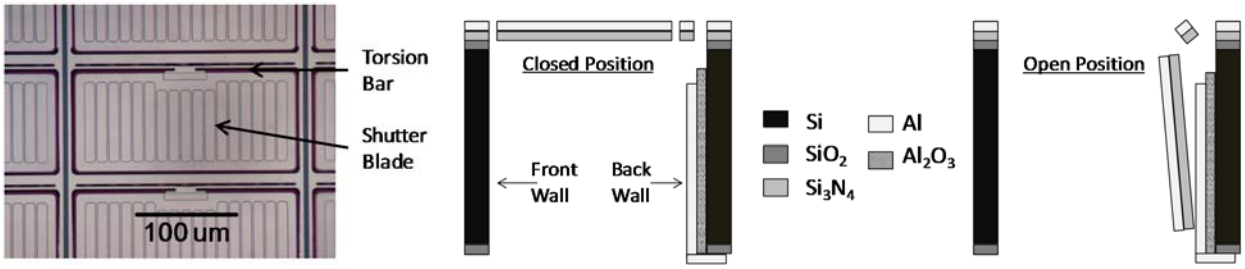

Figure 1(b)), the shutter is parallel with the wafer face. In the open position (

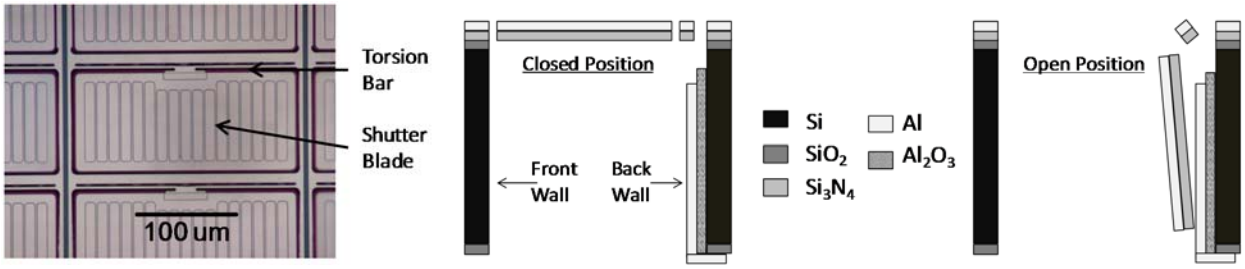

Figure 1(b)), the shutter torsion bar twists and the blade rotates open approximately ninety degrees and latches against the back wall. The microshutter torsion bar and blade are produced using surface micromachining processes on the front of the SOI wafer. The torsion bar and blade form a composite consisting of chemical vapor deposited Si_3N_4, which serves as the primary structural and dielectric layer, and electron beam deposited Al, which provides the front electrode contact. Processing is also conducted on the backside of the SOI wafer. Much of the silicon on the backside is removed using deep reactive ion etching. This creates wells behind each microshutter which they can rotate through. Atomic layer deposition techniques are used to deposit an Al_2O_3 coating to serve as an electrical insulator. Al is then deposited on the back walls creating a set of electrodes perpendicular to the front electrodes. This process electrically isolates column and row electrodes allowing applied voltages to uniquely address and open individual shutters.

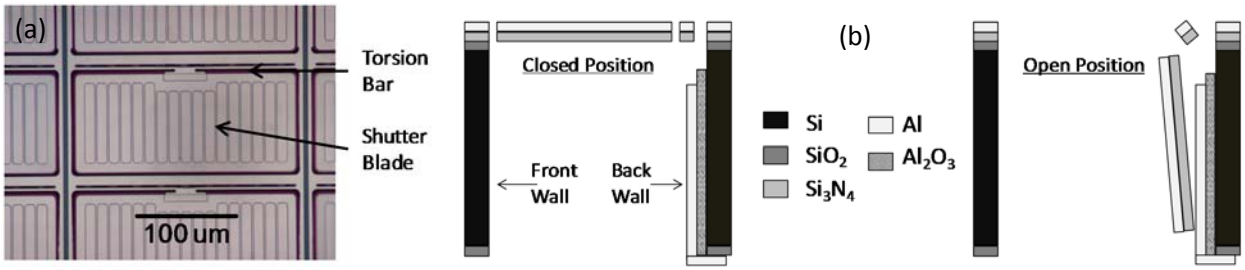

Figure 1. (a) Image of a fabricated microshutter array with torsion bars and blades highlighted. (b) Depiction of a cross section of a microshutter showing constitutive materials and the shutter in a closed and open configuration.

Cantilever beam test structures were fabricated along with the microshutter arrays for analysis of the mechanical properties of the as deposited materials. Mechanical properties were characterized using a custom designed micro-mechanical test system shown in Figure 2. The system consists of a FemtoTools capacitive force sensor equipped with a Tungsten wire probe for load measurement and a MicroEpsilon capacitive displacement gauge for displacement measurement. Cameras and microscope optics provide orthogonal views of the test specimen assisting with alignment of the test probe on the sample surface. The entire system is contained in an enclosure to help reduce the effect of air currents and thermal fluctuations on the measurements. LabVIEW was used to automate testing and for data acquisition. More details on the test system can be found elsewhere [(4)].

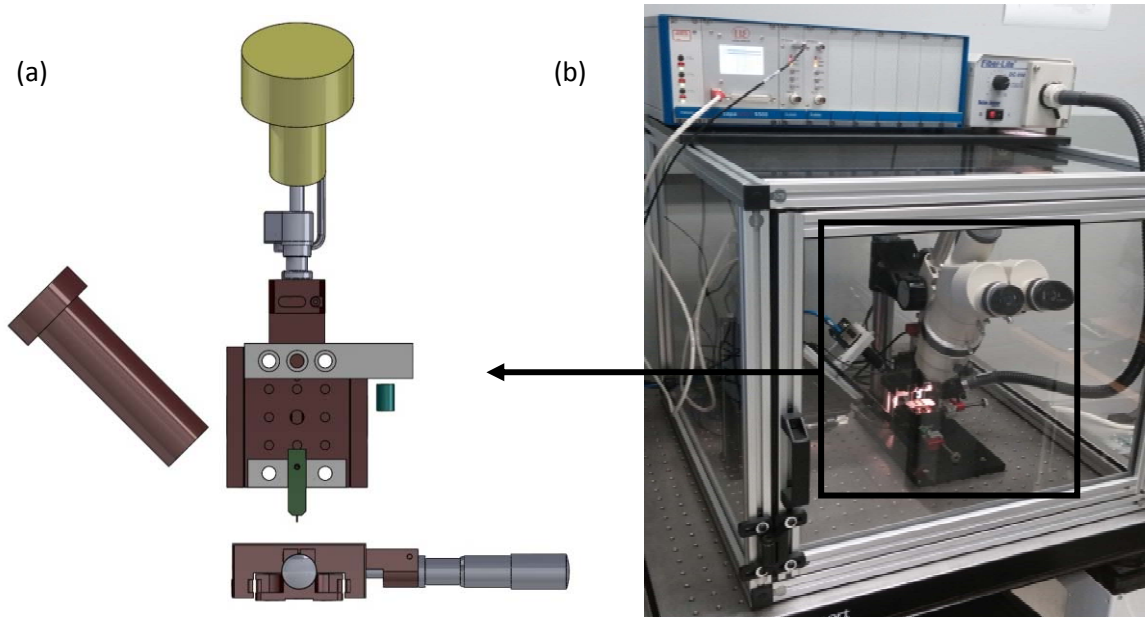

Figure 2. (a) Depiction of the main components of the mechanical test system including the FemtoTools capacitive force sensor (directly above lower sample stage), cameras and microscope optics (above and to the left), and the MicroEpsilon capacitive displacement gauge (fixed below the reference bar on the one axis stage). (b) Image of the test setup showing all the equipment mounted inside an enclosure to reduce air currents and thermal fluctuations.

A test system was also designed to measure the electromechanical response of microshutters. The test system consists of a vacuum chamber with feedthroughs to accommodate all 64 column and 128 row electrodes. Quartz windows were installed on opposite sides of the test chamber both centered on the microshutter array to allow for illumination and viewing from both directions. Light emitting diodes powered by a Gardasoft Vision LED light controller was used to provide both continuous and pulsed illumination of the microshutters. A Stanford Research function generator was used for producing AC signals of varying frequency and magnitude. For generating pulsed waveforms, a National Instruments multifunction data acquisition board with analog output capability was fed to a TEGAM high voltage amplifier. LabVIEW was used to conduct many experiments and for all image acquisition. To interface the microshutter array with the drive electronics, the array was indium bump bonded to a Si fan out board that was then bonded to a printed circuit board. Wire bonds connect the Si fan out board to the printed circuit board.

Results

To achieve electrostatic actuation at reasonable drive voltages, geometric modifications to existing magnetically actuated microshutters [(1) (2)] were pursued to lower the torsional stiffness of the shutters. The test systems described above were used to quantify how changes to the microshutter design altered torsional stiffness, while also assuring that mechanical integrity was not sacrificed. Figure 3 shows the torsional stiffness of magnetically actuated microshutters (500 nm Si_3N_4; 200 nm Al) compared to the torsional stiffness of the new electrostatic array (250 nm

Si_3N_4; 200 nm Al). By reducing the Si_3N_4 thickness by half in the electrostatic array design, the torsional stiffness is reduced by a factor of approximately four from 0.061 N/m to 0.015 N/m. Moreover, electromechanical tests performed on entire columns (64 shutters) of shutters have demonstrated that over 25,000 individual shutter latches can be performed without any observed structural failures.

Analytical and finite element models were developed to lend further credibility to the mechanical test results and to gain further understanding of the mechanical behavior. An analytical model for a bilayer rectangular beam in torsion, developed by Muskhelishvili [(5)], was applied to the analysis of the microshutters by assuming that the moment applied by the indentation probe was applied at the midpoint of the torsion bar. A finite element model, developed in COMSOL, was also used to simulate the mechanical properties of the microshutters. The model takes into account geometric non-linearities owing to the large rotation and assumes linear elastic material properties. Both models assume an elastic modulus of 150 GPa for the low stress Si_3N_4, based on experimental measurements of the modulus performed on Si_3N_4 cantilever beam test structures [(4)]. An elastic modulus of 70 GPa was assumed for Al. As shown in Figure 3, the predicted torsional stiffness of both models was in good agreement with the experimentally measured stiffness for both magnetically and electrostatically actuated designs. At the larger displacements, the finite element model appears to more accurately capture a slight deviation from the linear behavior predicted by the analytical model. This is likely due to the finite element models consideration of geometric non-linearity.

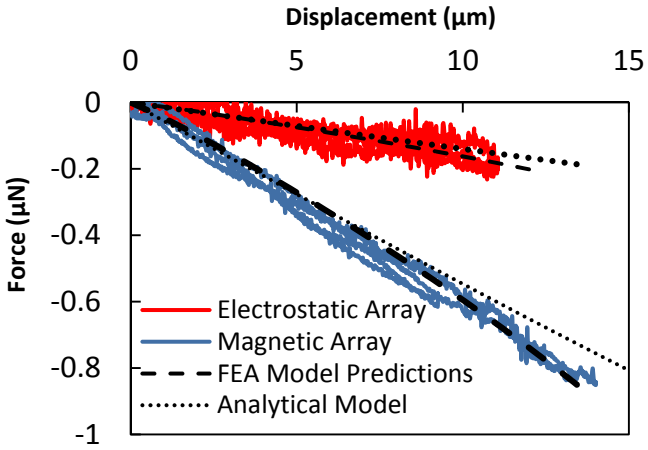

Figure 3. Mechanical test results showing the torsional stiffness of an electrostatically and magnetically actuated microshutter. The results of analytical and finite element models predicting the array's behavior are also shown.

The electrostatic actuation of microshutters is a balance between electrostatic forces driving the shutter open and mechanical forces resisting the shutter motion. The mechanical forces are well understood (at relatively low angles) based on the experimental and modeling data presented above. A modeling effort was also undertaken to gain a fuller understanding of the electrostatic forces. This modeling effort was carried out using COMSOL. Isolating the electrostatic forces is not practical experimentally since the electrostatic and mechanical forces are coupled. However, modeling can isolate the electrostatic forces by performing separate analyses of the shutter blade at fixed angles (rigid body rotation of the shutter blade free of stress generation) relative to the Si frame. Examples of this analysis procedure are shown in Figure 4(a), (b) and (c). Here a DC voltage is applied to the microshutter while maintaining the surrounding Si frame at ground potential. The difference in potential gives rise to the electrostatic forces. In Figure 4(a), (b) and (c) the normalized electric field generated from an applied voltage of 100V in each case is shown with the shutter oriented at fixed angles of 1, 20 and 50 respectively. These three cases indicate the dependence of the electric field on the angle of the blade. In particular, at lower angles the electric field is dominate towards the front (left side of graphic) and toward the back (right side of graphic) of the microshutter. This suggests that interactions with both the front and back wall are important at lower angles. At higher angles as the shutter

moves away from the front wall, interactions with the front wall become negligible and interactions with the back wall dominate.

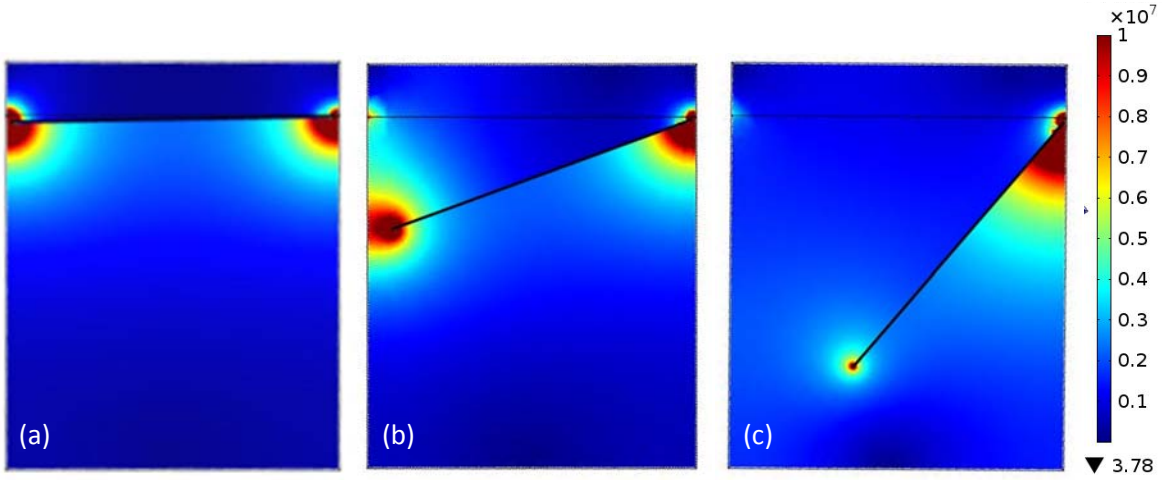

Figure 4. COMSOL modeling results depicting a cross section of the normalized electric field (V/m) as the shutter is opened to (a) 1° (b) 20° and (c) 50°.

A fuller picture of the electrostatic interactions is captured by Figure 5, which shows curves of constant voltage on a plot of torque (applied by the electrostatic forces) as a function of the shutter angle. From this plot, several things become clear. One, as the voltage applied to the shutter increases the torque exerted by the electrostatic forces on the shutter increases. Two, the electrostatic force acting on the shutter does not always increase as the shutter rotates toward the back wall. Instead, the net electrostatic force is strongest initially when the shutter is fully open (0° rotation) and again as the shutter approaches the back wall (40°+). In particular, as the shutter approaches 10° rotation a significant drop off in the torque exerted on the shutter is observed. This significant drop off is driven primarily by the shutters interaction with the front wall (see Figure 1 for clarification of front and back walls). In the closed position, the close proximity between the front wall and the shutter leads to a large entirely downward force or torque. But as the shutter rotates open, the top of the shutter blade is pulled upward while the bottom of the shutter blade is pulled downward. The top of the shutter blades interaction with the front wall leads to a drop off of the torque from 0° up to about 20°. As the shutter exceeds a 20° rotation, the influence of the back wall begins to dominate and the torque continues to increase as the shutter angle increases.

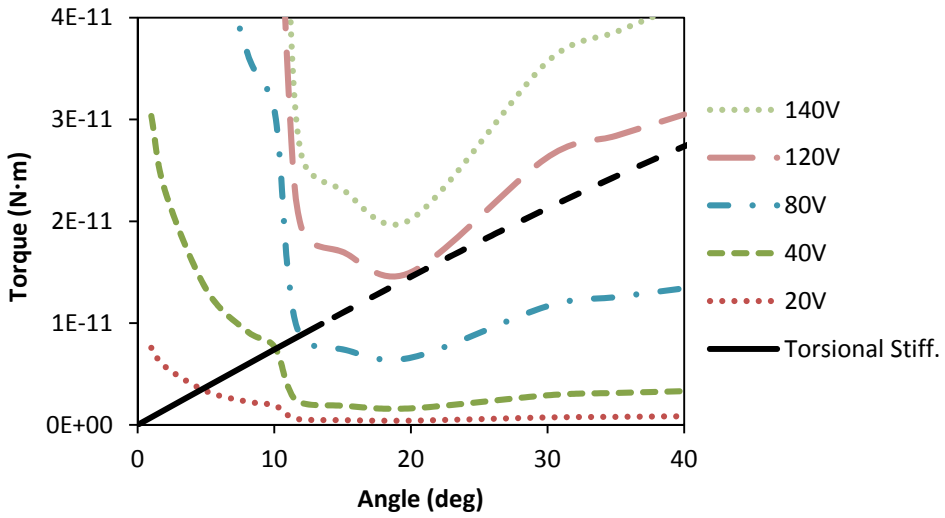

Figure 5. Plot of the predicted electrostatic torque exerted on the microshutter as a function of the opening angle for different applied voltages. Also shown in black is the measured mechanical torque required to open the microshutter to different angles (extrapolated to larger angles).

The torsional stiffness of the electrostatic array measured experimentally is also plotted in Figure 5. Note that for the sake of simplicity the torsional stiffness has been extrapolated to the larger angles (represented by the dotted black line) without taking into account geometric non-linearities. The intersection points between the torsional stiffness curve and the constant voltage curves represent equilibrium points in the DC actuation of a microshutter. At these points, the torque exerted on the shutter by the electrostatic forces is balanced by the restoring torque of the torsion bar.

Figure 6 shows the predicted displacement of the shutter based on the intersection point between the torsional stiffness curve and the constant voltage curves shown in Figure 5 (constant voltage curves were constructed for 10V, 20V, 30V, 40V and 50V though not all are shown in Figure 5 to improve clarity). Also shown in the figure is the average measured displacement of three microshutters as a function of the applied voltage (error bars represent one standard deviation of error). These measurements were taken by using an optical microscope to focus on the end of the microshutters as they displaced. Beyond 50V, it becomes difficult to resolve the displacement of the microshutter optically which is why the analysis stopped at that point. The microshutters were bowed slightly downwards causing the roughly 2 micron displacement at 0V. From the figure, it is clear that the measured and predicted displacements agree well. Both the model and experiment show a non-linear relationship between 0 and 20V with a downward concavity. Both models also show a change to upward concavity between 30 and 40V. While not shown in Figure 6, the predicted and measured pull in voltage also agrees well. The pull in voltage can be predicted for the microshutters based on the position of the electrostatic torque curves relative to the torsional stiffness shown in Figure 5. For any applied voltage above 120V, it is predicted that the electrostatic torque will always exceed the mechanical torque. Thus, the predicted pull in voltage is 120V. In practice, the majority of shutters were observed to have a pull in voltage between 100 and 120V.

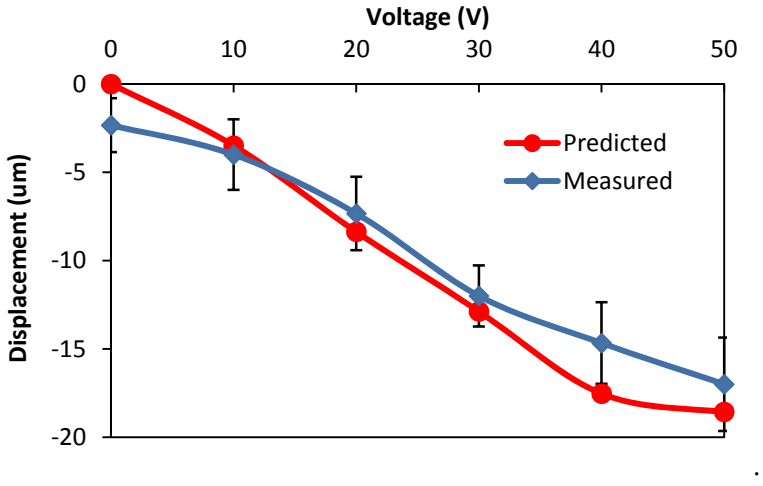

Figure 6. Plot of the measured and predicted displacement of a microshutter subjected to voltages ranging between 0 and 50V. The measured displacement is an average displacement of three measurements taken on different microshutters. The error bars represent one standard deviation of measured error.

The resonant behavior of the microshutters was also modeled by conducting an eigenfrequency analysis in COMSOL. The analysis explored taking advantage of resonance behavior to lower microshutter actuation voltage. The results of this analysis are shown in Figure 7 (a) and (b). The first resonant mode is a rotational mode about the shutter's hinge (Figure 7 (a)). This mode is predicted to occur at 2800 Hz. The rotational nature of this mode supports the idea that resonant actuation can be used to minimize actuation voltages. The second resonant mode

(Figure 7 (b)) sits comfortably above the first resonant mode at 6800 Hz. This mode is more lateral in motion and would not be conducive to microshutter actuation.

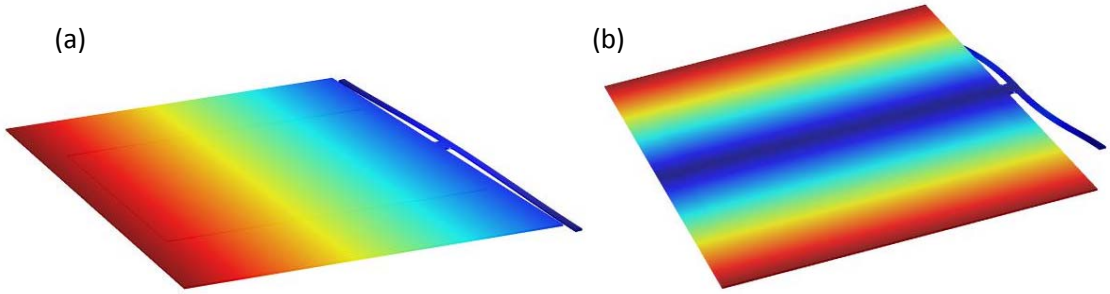

Figure 7. Results of an eigenfrequency analysis showing (a) the first torsional resonant mode occurring at 2800 Hz (b) the second lateral bending mode occurring at 6800 Hz.

The first resonant mode of the microshutters was further investigated experimentally. This analysis considered the effects of air dampening, which we suspected would significantly effect the dynamic behavior of microshutters. Experiments were run at different vacuum pressures to test this theory. Characterization of the microshutter behavior was performed by analyzing backlit images of microshutters taken using a strobe light designed to capture different phases of the shutter's motion relative to the drive signal. By analyzing the images taken at different frequencies and phases of motion using image thresholding tools available in LabVIEW, a full picture of the shutters displacement and phase was assembled. Figure 8(a), shows the same shutter subject to a 10V AC signal varying from 2900 Hz to 3500 Hz in 2 Hz increments at two different vacuum pressures. As evidenced from the figure, the displacement varies from a peak amplitude of 20 microns at 200 Pa to 43 microns at 5.4E-4 Pa. The large displacements generated at low vacuum pressures have been used to perform latching of microshutters with as little as a 0 to 10V AC signal applied to front electrodes and -15V applied to back electrodes. Note that the measured resonant frequency is occurring between 3100 and 3300 Hz for the microshutters analyzed. This differs from the 2800 Hz predicted by the eigenfrequency analysis. This discrepancy is likely a result of dimensional variations between the model and the shutter studied. Small dimensional variations can significantly shift the resonant frequency.

In addition to the large amplitude observed at low vacuum pressures, a distinct non-linear resonance behavior is observed at low vacuum pressures. This is evident from the asymmetric shape of the low vacuum pressure curve shown in Figure 8. This is highlighted by the sharp rise into the resonant state while scanning from low to high frequencies and the shift towards a lower center frequency. This behavior is likely due to a non-linear torsional stiffness, which becomes more apparent as the shutter opens to larger displacements. The subtle curvature of the FEA model predictions in Figure 3 demonstrates this effect. This is also supported by Figure 8 (b) where the resonant behavior of a shutter is shown at the same vacuum pressure (200 Pa) but subject to different AC voltages. For the higher 15V case, where the shutter displacement is larger, the non-linear characteristics become more apparent.

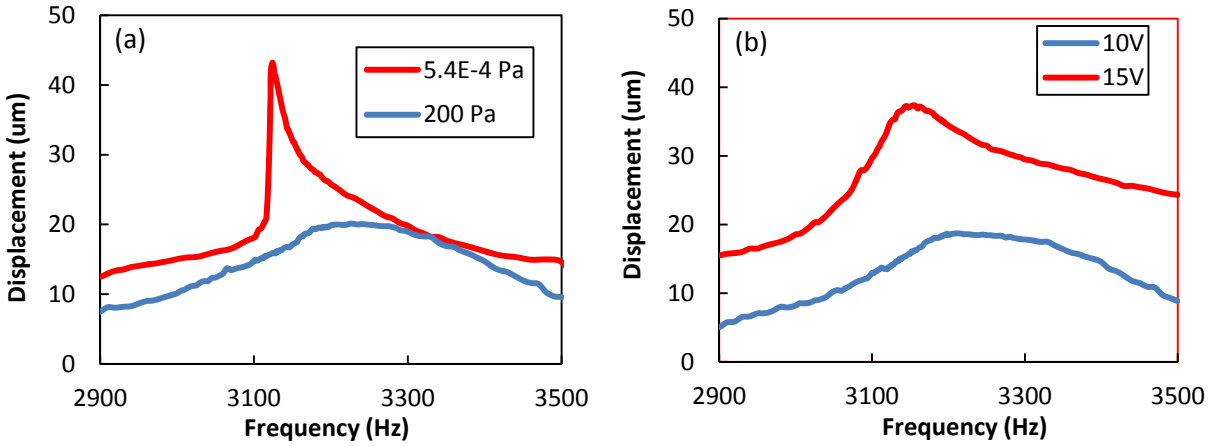

Figure 8. (a) Plot of the displacement of a microshutter as a 10V AC signal is swept from 2900 Hz to 3500 Hz at two different vacuum levels. (b) Displacement of the microshutter as 10V and 15V AC signals are applied over different frequencies both at a vacuum pressure of 200 Pa.

The experiments outlined above provide valuable insights into shutter behavior that become important when considering a 2-D addressing scheme. The scheme provides the mechanism to open or close individual microshutters. Figure 9 illustrates the addressing scheme used in this study. As shown in the figure, an AC resonant or pulsed signal is sent along shutter electrodes that run along array rows. Applying resonant or pulsed signals to shutter electrodes, while maintaining the substrate at ground, causes the shutters to open significantly. Negative DC potentials (with respect to ground) are then applied to electrodes that run along columns on the array back walls. Shutters at the intersection of the AC resonant or pulsed signals on shutter electrodes and DC potentials on the back wall electrodes are pulled in and latched against the back wall. The DC potential applied on the back wall electrodes is sufficient to keep the shutter latched against the back wall without application of voltage on the shutter electrode. Removing the potential on the back wall allows the shutters to close using the torsion bar's elastic restoring force.

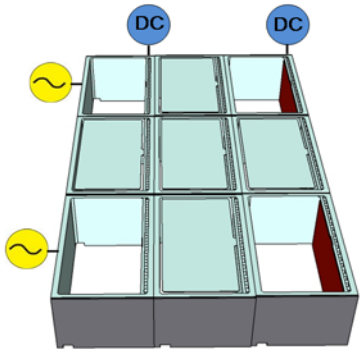

Figure 9. Depiction of 2D electrostatic addressing with AC resonant or pulsed voltages applied to row electrodes and DC voltages applied to column electrodes on shutter back walls.

Figure 10 illustrates the 2-D addressing concept using AC resonant actuation. This experiment was performed in air. Two shutter electrodes (top and bottom row in Figure 10) were supplied with a 0 to 70V, 1.9 kHz AC signal. This signal causes the shutters to enter resonance and swing through large displacements (2nd image). Maximum displacement of the shutter was observed by using strobe illumination at a set phase with respect to the AC signal. A DC potential of -35V DC was then applied to the back wall electrodes of column three causing the shutters at the intersection of the AC and DC potential to latch (3rd image). Then, a DC potential of -35V DC was applied to the column one back electrodes causing the targeted shutters to latch (4th image). The AC potential was then removed

and all the shutters remained latched with just the application of the DC voltage (5th image). The DC voltage was then removed sequentially on columns three (6th image) and one (7th image) causing the shutters to close. This particular shutter array had light shields (segments of material that sit above the microshutter and prevent light from leaking through from gaps between the shutter and the walls). The shutter runs into the light shields during resonant actuation and this interaction likely dampens shutter motion and requires larger actuation voltages compared to shutters without light shields.

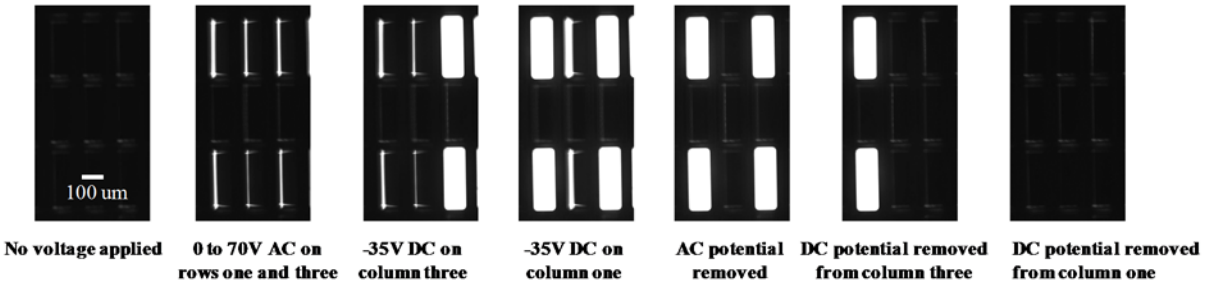

Figure 10. Sequence of images that demonstrate resonant electrostatic actuation of microshutters. A 0 to 70V, 1.9 kHz AC signal applied to row electrodes one and three places the shutters in resonance. -35V DC applied to columns three and one sequentially latched the shutters. Removing the DC potential from the back electrodes allows the shutters to close.

Pulsed addressing is depicted in Figure 11. Here, -25V DC is first applied to column back electrodes one and three (1st image). No change in the shutters is observed with the application of the -25V DC because the electrostatic force is almost negligible with the roughly 100 micron distance between the shutter and the back electrode. By applying a 100V square pulse with 200 microsecond duration to shutter electrodes along rows one and three, all four shutters subject to the pulse and the DC potential latch and remain latched due to the continued application of the DC voltage on back wall electrodes (2nd image). DC voltages are then sequentially removed from column back electrodes one and three causing the shutters to close (3rd and 4th images).

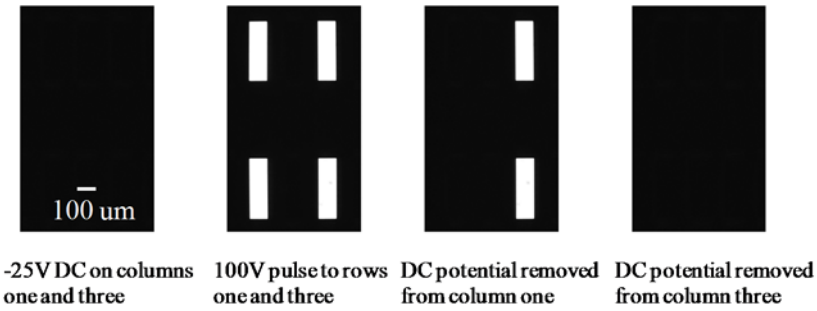

Figure 11. Images demonstrating the pulsed electrostatic actuation of microshutters. -25V DC is first applied to columns one and three before applying a 100V pulse to rows one and three. The 100V pulse causes shutters with the additional -25V DC applied to latch. The DC voltages can then be removed to close the shutters.

Conclusions

In this work, a microshutter based on rotational electrostatic actuation is designed, developed, and evaluated. The results demonstrate a resonant and a pulsed 2-D addressing scheme which are both capable of actuating, latching, and releasing individual microshutters. Both schemes require less than 150V and low currents to operate making them compatible with existing high voltage integrated circuit drivers. This is a significant advancement compared to

previous magnetically actuated microshutter arrays, because electrostatic actuation drastically simplifies the operation of these devices. New electrostatically actuated microshutters require less support hardware for operation, are easily scalable, and can operate much faster. These advancements may allow a broader adoption of rotational microshutter technology for applications requiring high contrast and fill factors.

Acknowledgements

The authors would like to thank Nick Costen, Bing Guan, and George Manos for assistance packaging the microshutter arrays. We are also grateful for electrical measurements performed by Frederick Wang and modeling advice provided by Ed Aguayo.

References:

1. *Microshutter Array development for the James Webb Space Telescope.* Li, M J. 2005. Proc. of SPIE. Vol. 5650.

2. *MEMS Microshutter Array System for James Webb Space Telescope.* Li, M J. 2008. Proc. of Hilton Head Workshop.

3. *Development of Microshutter Arrays for Ground-Based Instruments.* Motohara, K. s.l. : Proc. Instrumentation of Extremely large Telescopes, 2005.

4. *Mechanical Behavior of Microelectromechanical Microshutters.* Burns, D E, Jones, J S and Li, M J. s.l. : Proc. of SPIE. Vol. 9170.

5. Muskhelishvili, N I. *Some Basic Problems of the Mathematical Theory of Elasticity.* Groningen, Netherlands : Noordhoff Ltd, 1963. pp. 623-626.